

# Proposal for an extreme-ultraviolet Auger laser at 63.8 nm in Cs III

D. J. Walker, R. G. Caro,\* and S. E. Harris

*Edward L. Ginzton Laboratory, Stanford University, Stanford, California 94305*

Received April 30, 1986; accepted July 21, 1986

A system is proposed in which Cs atoms photoionized by soft x rays from a laser-produced plasma undergo selective Auger decay, causing inversion and lasing at 63.8 nm in Cs III. Rate-equation calculations show that lasing should occur when a small (1-J) 532-nm pump laser is used. A similar system in Rb III is briefly discussed.

It has been shown that large densities of highly excited atoms can be produced as a result of photoionization by soft x rays emitted from a laser-produced plasma.<sup>1,2</sup> By this technique, population inversions have been produced, and lasing in the visible and near-ultraviolet regions of the spectrum has been observed.<sup>3,4</sup> In this paper we propose a system in which these x rays would photoionize Cs vapor, producing Cs II  $4d^9 5s^2 5p^6 6s$  ions. These ions would then undergo rapid, selective Auger decay, resulting in an inversion of the Cs III  $4d^{10} 5p^4 5s^2 6s$  configuration with respect to the Cs III  $4d^{10} 5p^5 5s^2$  configuration and lasing at 63.8 nm. A similar system in which the Rb III  $3d^{10} 4p^4 4s^2 5s$  configuration is inverted with respect to the Rb III  $3d^{10} 4p^5 4s^2$  configuration, resulting in gain at 49 nm, will be discussed briefly.

The key point in identifying systems such as those described in this paper is to note that Auger decay will be rapid and therefore selective when the two interacting electrons both make strong dipole transitions, one to a bound level and one to the continuum, and when the average distance between these electrons is small and hence the Coulomb interaction is large. This occurs when the two interacting electrons belong to the same  $n$  shell and when they have opposite spin. In this sense the present proposal is similar to that of the Zn III system of Mendelsohn and Harris.<sup>5</sup> The present system has the additional advantage that the cross section for  $d$ -shell photoionization is larger than that of the other shells and therefore should be more efficient and less sensitive to electron deexcitation than was the Zn system.

We note that the use of Auger processes to create inversions in the extreme ultraviolet has been suggested earlier by McGuire<sup>6</sup> and Krolik and Shapiro<sup>7</sup> and has been demonstrated at visible wavelengths by Bokor *et al.*<sup>8</sup>

An energy-level diagram for the suggested Cs III laser system is shown in Fig. 1. The laser-produced x rays are assumed to have a blackbody spectral distribution with a temperature of 35 eV. Photoionization of Cs I by these x rays primarily produces  $4d$  vacancies. According to the prediction of the RCN/RCG code,<sup>9</sup> 83% of these vacancies Auger decay to the Cs III  $4d^{10} 5s^2 5p^4 6s$  configuration with an average Auger rate of  $4 \times 10^{13} \text{ sec}^{-1}$ . Of these, 31% are predicted to go into the upper laser level  $4d^{10} 5s^2 5p^4 6s \ ^2D_{5/2}$ , therefore giving a total predicted yield to this level of 26%. About 1% of the initial vacancies are predicted to decay to the lower laser level  $4d^{10} 5s^2 5p^5 \ ^2P_{3/2}$ , and therefore the pre-

dicted degeneracy normalized inversion  $[N_u - (g_u/g_L)N_L]$  is about 24.5. This prediction is confirmed by experimental Auger electron spectroscopy.<sup>10</sup> In Fig. 1, the level positions of Cs I and the lower two configurations of Cs II are taken from the tables of Moore.<sup>11</sup> The energy of the laser transition at 63.8 nm is taken from Epstein and Reader,<sup>12</sup> and the RCN/RCG code is used for the other level positions as well as for the calculated Auger rates and oscillator strengths.

In Rb III similar calculations predict that Auger decay should result in a degeneracy normalized inversion of the Rb III  $3d^{10} 4s^2 4p^4 5s \ ^2S_{1/2}$  level relative to the Rb III  $3d^{10} 4s^2 4p^5 \ ^2P_{3/2}$  level of a factor of 4.5 and that the wavelength of this transition is 49 nm. Experimental evidence supporting this prediction has been reported by Menzel and Mehlhorn.<sup>13</sup>

Although the photoionization process is predicted to produce a substantial inversion on the Cs III  $4d^{10} 5s^2 5p^4 6s \ ^2D_{5/2} - 4d^{10} 5s^2 5p^5 \ ^2P_{3/2}$  transition, many secondary processes can act to diminish or even destroy the inversion. To examine this problem, a rate-equation model has been used to predict the populations in a variety of levels in Cs I, Cs II, and Cs III under the conditions in which it is proposed to observe lasing on the 63.8-nm transition. The processes listed in Table 1 are those that have been considered of importance and that have been included in the model. The detailed mechanics of the rate-equation model are described elsewhere.<sup>14</sup>

Processes (1) and (2) of Table 1 are the photoionization and Auger decay processes that lead to population of Cs II and Cs III levels. The photoionization cross sections for the  $4d$ ,  $5s$ , and  $5p$  subshells of Cs I are obtained from the experimental work of Hecht.<sup>15</sup> The photoionization cross section for the  $6s$  subshell was obtained by an extrapolation of the data of Marr.<sup>16</sup> The branching ratios for determining the distribution of the products of Auger decay among the Cs III levels were calculated with the RCN/RCG code. The RCN/RCG calculations also show that the near degeneracy of the Cs II  $4d^9 5s^2 5p^6 6s$  and Cs II  $4d^9 5s^2 5p^6 5d$  configurations does not result in appreciable mixing between levels of the Cs II  $4d^9 5s^2 5p^6 5d$  configuration and levels of Cs II  $4d^9 5s^2 5p^6 6s$  configuration that undergo Auger decay; hence this near degeneracy does not affect the Auger branching ratios. We note that one ambiguity exists: calculations show that the Cs III  $4d^{10} 5p^6 6s$  configuration is nearly degenerate with the Cs II  $4d^9 5s^2 5p^6 6s$  configuration, and we are unable to predict which has the higher energy. Thus, if the Cs III configura-

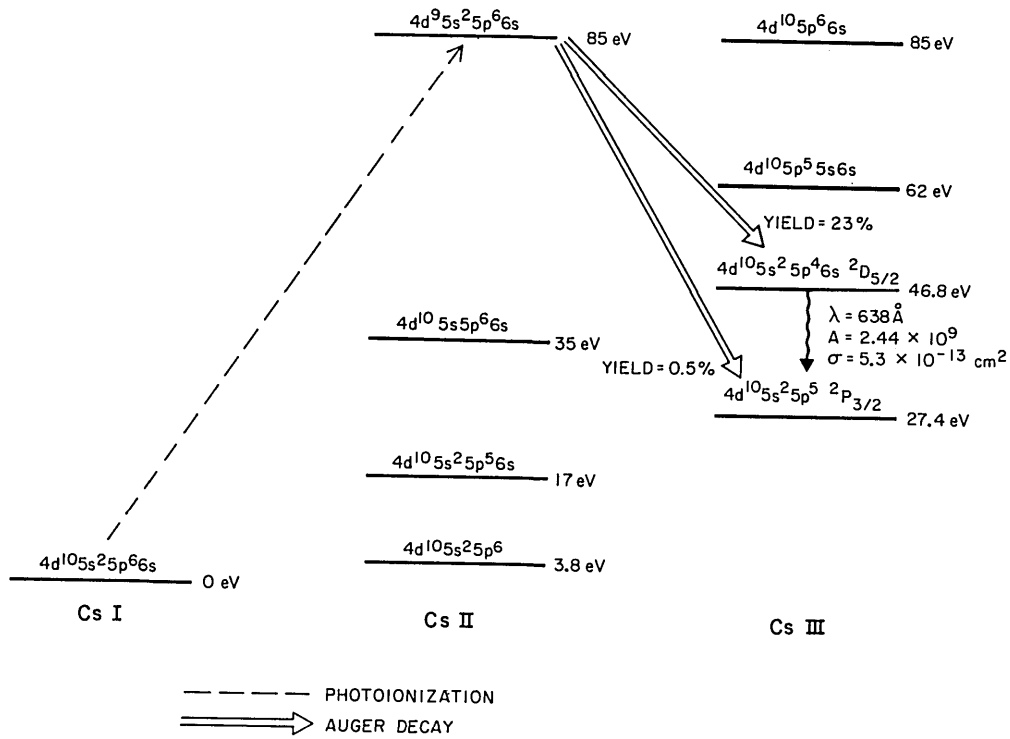


Fig. 1. Cesium Auger laser system.

**Table 1. Processes Included in Rate-Equation Model**

- (1) Photoionization from Cs I  $4d^{10}5s^25p^66s$  to Cs II  $4d^{10}5s^25p^6$   
 $4d^{10}5s^25p^66s$   
 $4d^95s^25p^66s$
- (2) Auger decay from Cs II  $4d^95s^25p^66s$  to Cs III  $4d^{10}5s^25p^46s$   
 $4d^{10}5s^25p^45d$   
 $4d^{10}5s^25p^5$   
 $4d^{10}5p^55s6s$
- (3) Radiative decay of Cs III  $4d^{10}5p^45s^26s$  to Cs III  $4d^{10}5s^25p^5$   
 $4d^{10}5p^45s^25d$
- (4) Gain depletion by ASE
- (5) Electron double ionization of Cs I  $4d^{10}5s^25p^66s$
- (6) Electron single ionization of Cs I  $4d^{10}5s^25p^66s$   
Cs I  $4d^{10}5s^25p^66p$   
Cs II  $4d^{10}5s^25p^6$   
Cs II  $4d^{10}5s^25p^66s$   
Cs III  $4d^{10}5s^25p^5$   
Cs III  $4d^{10}5s^25p^46s$
- (7) Electron excitation of Cs I  $4d^{10}5s^25p^66s \leftrightarrow 4d^{10}5s^25p^66p$   
Cs II  $4d^{10}5s^25p^6 \leftrightarrow 4d^{10}5s^25p^66s$   
Cs III  $4d^{10}5s^25p^5 \leftrightarrow 4d^{10}5s^25p^46s$

tion lies below the Cs II configuration, it will be populated by Auger decay, whereas, if it is above, it will not. This uncertainty has a small effect on the Auger branching ratios.

Process (3) of Table 1 is included to account for filling of the lower laser level by spontaneous radiative decay from all levels of Cs III that have significant Auger yield. The designations of these levels together with their calculated branching ratios and radiative decay times are listed in Table 2.

Falcone<sup>17</sup> has recently noted that, in high-gain super-

fluorescent systems, particularly those with low aspect ratio, amplified spontaneous emission (ASE), process (4) of Table 1, plays an important role in determining the magnitude and duration of the gain of the system. This is because as the population inversion and the gain rise, spontaneous emission in directions other than the lasing direction causes other pumped atoms to radiate in random directions. This reduces the system gain without contributing to the output signal. For the rate-equation model used here, we assume a cylindrical volume of length  $L$ , diameter  $D$ , and aspect ratio  $L/D$  and calculate the stimulated lifetime of upper-laser-level atoms in the presence of the photon field of the surrounding atoms.

Processes (1)–(4) of Table 1 deal with the effects of interactions between photons and Cs atoms and ions; processes

**Table 2. Auger Branching Ratios and Decay Times of Levels That Decay Radiatively to the Lower Cs III Laser Level**

Designation	Auger Yield (%) from Cs II	Radiative Decay Time to Lower Laser Level (nsec)	Total Radiative Decay Time (nsec)
Cs III $4d^{10}5s^25p^46s \ ^2D_{5/2}$	23.0	0.41	0.41
$4d^{10}5s^25p^46s \ ^2S_{1/2}$	11.0	0.38	0.05
$4d^{10}5s^25p^46s \ ^4P_{1/2}$	6.8	2.0	2.0
$4d^{10}5s^25p^46s \ ^4P_{5/2}$	4.7	2.7	2.7
$4d^{10}5s^25p^46s \ ^4P_{3/2}$	4.0	1.1	1.1
$4d^{10}5s^25p^46s \ ^2P_{3/2}$	3.9	0.45	0.45
$4d^{10}5s^25p^46s \ ^2P_{1/2}$	3.2	0.47	0.26
$4d^{10}5s^25p^45d^2S_{1/2}$	2.6	0.053	0.03
$4d^{10}5s^25p^45d^4P_{3/2}$	2.2	1.0	1.0

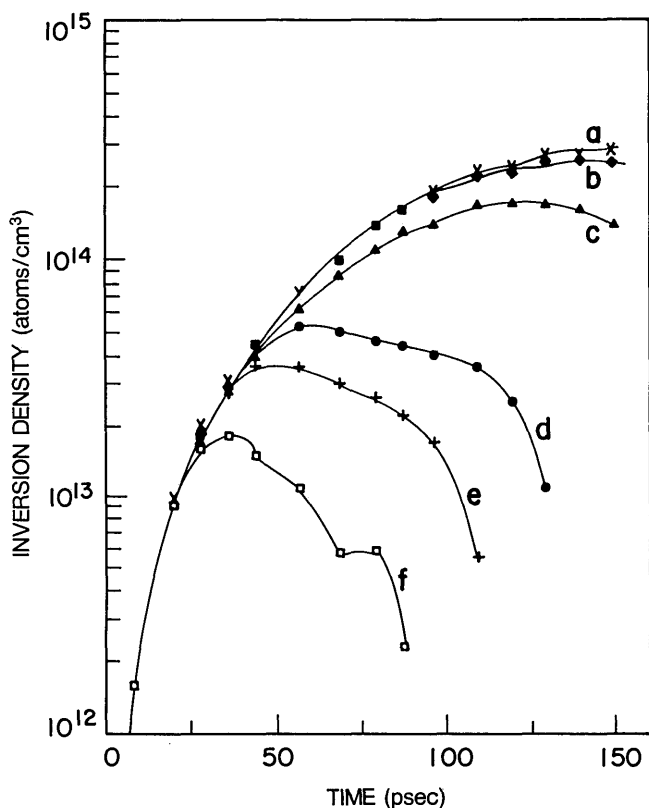


Fig. 2. Inversion density versus time. Curve a, no electrons, radiative decay, or ASE; curve b, no radiative decay or ASE; curve c, no ASE; curve d, aspect ratio = 32; curve e, aspect ratio = 8; curve f, aspect ratio = 1.

(5)–(7) are included to take into account the dominant electron–atom and electron–ion collisional interactions. For example, double electron ionization of Cs I produces lower-laser-level atoms of Cs III. Also, if sufficiently intense, electron deexcitation may deplete the upper-laser-level population.

We model the proposed laser system assuming a 1-J 532-nm laser of pulse length 100 psec FWHM focused onto a Ta target in a 3-cm line focus. We assume a Cs-vapor density of  $2 \times 10^{16}$  atoms/cm<sup>3</sup> (the large absorption cross section<sup>18</sup> at 63.8 nm of Cs I of  $\sigma = 3 \times 10^{-17}$  cm<sup>2</sup> precludes higher-density length products), a soft-x-ray blackbody temperature of 35 eV, and 10% conversion of laser energy to x-ray energy. The gain axis is taken to be 1 mm from the target.

The predictions of our model are illustrated in Fig. 2, where we plot the inversion density of the 63.8-nm laser transition as a function of time from the start of the pump laser pulse. In order to separate the relative importance of the processes listed in Table 1, we plot several curves. For curve a the model includes only the primary photoionization and Auger decay. To obtain curve b, electron processes (5)–(7) are added, whereas for curve c the effect of radiative cascades is also included. Curves d–f represent the predictions of the model for several different aspect ratios when all the processes in Table 1 are included. By comparing curves a and b, we can see the relative unimportance of electron processes on the predicted inversion. The reason for this is that, for the electron velocities and cross sections involved, the probability of the occurrence of processes (5)–(7) is small

during the 100-psec duration of the laser pulse. For longer pump pulses, these processes would become important. Curve c shows the effect of cascades from the levels listed in Table 2. The effect of these cascades is to reduce the duration and magnitude of the inversion by filling the lower laser level more quickly. Curves d–f show that ASE can dramatically reduce the inversion in systems of small aspect ratio, whereas for large aspect ratio the effect is smaller.

At a temperature of 270°C, corresponding to a Cs-vapor density of  $2 \times 10^{16}$  atoms/cm<sup>3</sup>, the Doppler width of the 63.8-nm transition is 0.23 cm<sup>-1</sup>. A calculation of the hyperfine splitting of the upper laser level using Sobel'man's<sup>19</sup> and RCN/RCG wave functions indicates that the hyperfine splitting is larger than the Doppler width and that only a single hyperfine component falls under the Doppler width. Assuming that each hyperfine component is populated in proportion to its degeneracy, the largest hyperfine component of the  $4d^{10}5s^25p^46s^2D_{5/2}$  level receives 1/3.7 of the total population. (Therefore the Auger yield to this particular component is 6.2%.) This, along with the gain cross section of  $5.6 \times 10^{-13}$  cm<sup>2</sup> and the curves of Fig. 2, therefore implies a maximum gain on the 63.8-nm transition of  $\exp(21)$  at an aspect ratio of 32. It should be noted that the model predictions are insensitive to the exact temperature of the soft-x-ray blackbody—the inversion drops to half of its peak value at 15 and 75 eV.

To summarize, we have suggested a method of using selective Auger decay to produce population inversion and gain in Cs III at 63.8 nm. Rate-equation calculations show that a 100-psec, 1-J pulse of 532-nm light should produce superfluorescent gain. An analogous system in Rb III at 49 nm was also briefly discussed.

## ACKNOWLEDGMENTS

The authors acknowledge important discussions with J. Reader, R. W. Falcone, A. J. Mendelsohn, and J. F. Young.

The research here was supported by the Strategic Defense Initiative Organization, the U.S. Army Research Office, the U.S. Air Force Office of Scientific Research, the U.S. Office of Naval Research, and the Lawrence Livermore National Laboratory.

\* Present address, Summit Technology, Inc., 150 Coolidge Avenue, Watertown, Massachusetts 02171.

## REFERENCES AND NOTES

1. R. G. Caro, J. C. Wang, R. W. Falcone, J. F. Young, and S. E. Harris, *Appl. Phys. Lett.* **42**, 9 (1983).
2. R. G. Caro, J. C. Wang, J. F. Young, and S. E. Harris, *Phys. Rev. A* **30**, 1407 (1984).
3. W. T. Silfvast, J. J. Macklin, and O. R. Wood II, *Opt. Lett.* **8**, 551 (1983).
4. H. Lundberg, J. J. Macklin, W. T. Silfvast, and O. R. Wood II, *Appl. Phys. Lett.* **45**, 335 (1984).
5. A. J. Mendelsohn and S. E. Harris, *Opt. Lett.* **10**, 128 (1985).
6. E. J. McGuire, *Phys. Rev. Lett.* **35**, 884 (1975).
7. J. H. Krolik and P. R. Shapiro, *J. Phys. B* **16**, 4687 (1983).
8. J. Bokor, R. R. Freeman, and W. E. Cooke, *Phys. Rev. Lett.* **48**, 1242 (1982).
9. R. D. Cowan, *The Theory of Atomic Structure and Spectra* (California U. Press, Berkeley, Calif., 1981), Secs. 8-1, 16-1, and 18-7.

10. H. Aksela and S. Aksela, *Phys. Rev. A* **28**, 2851 (1983).
11. C. E. Moore, *Atomic Energy Levels, Vol. III* (National Bureau of Standards, Washington, D.C., 1971), pp. 124–130.
12. G. L. Epstein and J. Reader, *J. Opt. Soc. Am.* **66**, 590 (1976).
13. W. Menzel and W. Mehlhorn, in *Inner-Shell and X-Ray Physics of Atoms and Solids*, D. J. Fabian, H. Kleinpoppen, and L. M. Watson, eds. (Plenum, New York, 1981).
14. R. G. Caro and J. C. Wang, *Phys. Rev. A* **33**, 2563 (1986).
15. M. H. Hecht, "Soft x-ray photoionization cross sections: measurement and applications," Ph.D. dissertation (Department of Applied Physics, Stanford University, Stanford, Calif., 1983).
16. G. V. Marr, *Photoionization Processes in Gases* (Academic, New York, 1967), p. 115.
17. R. W. Falcone, Department of Physics, University of California, Berkeley, California 94720 (personal communication).
18. C. E. Theodosiou and W. Fielder, Jr., *J. Phys. B* **15**, 4113 (1982).
19. I. I. Sobel'man, *An Introduction to the Theory of Atomic Spectra* (Pergamon, Oxford, 1972), Chap. 6.